

The Fabrication and Characterization of Piezoelectric PZT/PVDF Electrospun Nanofiber Composites

Regular Paper

Ji Sun Yun^{1*}, Chun Kil Park¹, Young Hun Jeong¹, Jeong Ho Cho¹, Jong-Hoo Paik¹, Sun Hong Yoon² and Kyung-Ran Hwang³

¹ Electronic Materials Convergence Division, Korea Institute of Ceramic Engineering and Technology, Jeonju, South Korea

² IT Application Research Center, Korea Electronics Technology Institute, Jeonju, South Korea

³ Biomass and Waste Energy Laboratory, Korea Institute of Energy Research, Daejeon, South Korea

*Corresponding author(s) E-mail: susubin@kicet.re.kr

Received 09 October 2015; Accepted 09 February 2016

DOI: 10.5772/62433

© 2016 Author(s). Licensee InTech. This is an open access article distributed under the terms of the Creative Commons Attribution License (<http://creativecommons.org/licenses/by/3.0>), which permits unrestricted use, distribution, and reproduction in any medium, provided the original work is properly cited.

Abstract

Piezoelectric nanofiber composites of polyvinylidene fluoride (PVDF) polymer and PZT ($\text{Pb}(\text{Zr}_{0.53}\text{Ti}_{0.47})\text{O}_3$) ceramics were fabricated by electrospinning. The microstructure of the PZT/PVDF electrospun nanofiber composites was characterized using X-ray diffraction (XRD), scanning electron microscopy (SEM) and transmission electron microscopy (TEM). The tensile properties (stress-strain curves) and electrical properties (P-E hysteresis loops) of the PZT/PVDF electrospun nanofiber composites were investigated as a function of PZT content from 0 wt% to 30 wt%. The results demonstrated that a PZT content of 20 wt% had enhanced tensile and piezoelectric characteristics.

Keywords PZT, Nanofiber Composites, Dielectric Function, Fibre Technology, Electrospinning

1. Introduction

PZT (lead zirconate titanate, $\text{Pb}(\text{Zr}_x\text{Ti}_{1-x})\text{O}_3$), ceramic is a typical piezoelectric material that can interconvert electric

energy to mechanical energy. Due to the piezoelectric characteristic of the material, it is widely used in various applications, such as sensor and actuator materials, non-volatile ferroelectric memory devices, micro-electromechanical systems (MEMS) and nanogenerators [1-4]. Sintered bulk PZT ceramics are brittle materials and there is a growing demand for flexible PZT nanofiber materials [5-8].

The electrospinning process, one of the most common methods to fabricate fibrous PZT, is probably the simplest technology for manufacturing nanofibers with an exceptionally long length, uniform diameter and diversified composition [9]. The formation of nanofibers by electrospinning is based on the uniaxial stretching of a viscoelastic jet derived from a polymer solution or melted under high voltages. PZT electrospun nanofibers from a sol-gel solution need a sintering process at over 650 °C for growing a perovskite crystal structure [8]. During this sintering process, PZT nanofibers become less flexible. To overcome this disadvantage, the technology for fabricating nanofibers of ceramic and polymer composites needs to be developed to eliminate the sintering process after electrospinning.

Polyvinylidene fluoride (PVDF) polymers are good candidates for fabricating PZT and polymer composites. PVDF polymers are classified as homopolymers and copolymers. The PVDF homopolymer is a strong engineering fluoropolymer. The PVDF copolymers are similar to homopolymers in purity and chemical resistance, but also have chemical compatibility in high pH solutions, increased impact strength at ambient and low temperatures and increased clarity. Copolymers of PVDF are used in piezoelectric and electrostrictive applications. One of the most commonly used copolymers is P(VDF-trifluoroethylene) and another is P(VDF-tetrafluoroethylene). PVDF copolymers improve the piezoelectric response by improving the crystallinity of the material. P(VDF-TrFE) copolymers exhibit ferroelectric, piezoelectric and structural properties that may be superior to those of PVDF. In this paper, by PVDF we are referring to P(VDF-trifluoroethylene).

In this study, PZT/PVDF electrospun nanofiber composites were prepared from a mixture of sintered PZT ceramic powder and PVDF polymer dissolved in dimethylformamide (DMF) and acetone. We then analysed the mechanical and electrical characteristics of the PZT/PVDF electrospun nanofiber composites with various levels of PZT content and found that the optimal PZT content was 20 wt% for desirable tensile and piezoelectric characteristics. The mechanical properties of the piezoelectric nanofiber films, such as tensile strength and Young's modulus, have an effect on the blocking force and durability of the final actuators [11].

2. Experimental Details

The P(VDF-TrFE) copolymer powder (Measurement Specialties) with VDF 75 % and TrFE 25 % was dissolved in a DMF (dimethylformide, Sigma-Aldrich, 99.5 %) and acetone (Sigma-Aldrich, 99.5 %) mixture at room temperature for one day. The molar composition of the PVDF polymer solution was as follows: PVDF : DMF : acetone = 0.4 : 1 : 1. Sintered PZT ceramic powder (Sunnytec Co., P-5H) at 1,150 °C for 30 min was added to the PVDF polymer solution and then stirred for three days. The electrospinning conditions of the PZT/PVDF mixture were as follows: the distance between the tip of the syringe and the collector was 10 cm, the syringe tip diameter was 23 G (nominal outer diameter: 0.6414 mm, nominal inner diameter: 0.337 mm, nominal wall thickness: 0.1524 mm), the feeding rate of the solution was 30 $\mu\ell$ /min and the electrospinning voltage was 15–18 kV.

For analysing the electrical properties, PZT/PVDF nanofiber film with dimensions of 1 cm (W) \times 5 cm (L) \times 0.5 cm (T) was fixed to the bottom electrode film using a thermosetting epoxy adhesive and the sheet was then slightly heated at 70 °C under 80 bar for 30 min. The top electrode was also applied to the PZT/PVDF nanofiber film by the same process. The bottom and top interdigitated electrodes were

made using a photoresist-and-etch process on commercially available copper-clad polyimide film.

The crystal structure and surface morphology of the PZT/PVDF nanofibers were observed using XRD (Rigaku corporation, D/max 2200V/PC), SEM (Jeol, JSM-6700F) and TEM (Jeol / JEM-4010). The polarization-electric field (P-E) hysteresis loops were measured using a ferroelectric test system (Radiant P-LC-K) at room temperature. To prepare samples for measuring the tensile properties, PZT/PVDF nanofiber films were prepared with dimensions of 1 cm (W) \times 7 cm (L) \times 0.5 cm (T). The tensile properties of the PZT/PVDF nanofiber composite films were studied using a tensile tester (Instron 5564). The test speed was set to 0.5 N mm/min.

3. Results and Discussion

The effect of the PZT content on the morphology and average diameters of the PZT/PVDF nanofibers is shown in Fig. 1. The average diameter was calculated and plotted for the PZT/PVDF nanofibers, based on the SEM images. The density of the PZT/PVDF mixture solution increased with an increasing PZT content. The SEM images showed that the morphology of the PZT/PVDF nanofibers becomes gradually stiffer with an increasing PZT content. The diameter of the PZT/PVDF nanofibers increased to a PZT content of 10 wt% and the diameters of the PZT 20wt% and 30 wt% samples decreased. Due to PZT particles aggregating within the nanofiber regions, as shown in Fig. 2(a), the diameter of the PZT/PVDF nanofiber is larger than that of the PVDF nanofiber. However, during electrospinning, the aggregation of some extra PZT particles seems to form clusters on the nanofiber surfaces and a maximum diameter was found for an intermediate percentage. This tendency was clearly observed in the PZT/PVDF nanofibers with 30 wt% PZT. In the nanofibers, PZT ceramic powders tended to clump together instead of forming a composite with the PVDF polymer.

The TEM image and optical image of the PZT/PVDF nanofiber films with a PZT content of 20 wt% are shown in Fig. 2. In the TEM image (Fig. 2(a)) of the PZT/PVDF nanofibers with a PZT content of 20 wt%, the agglomeration of PZT particles (black spots) can be observed in the volume of the nanofiber. Due to the repulsion force of induced electrical charges on the PVDF, these PZT particles were directed towards the inside of the PVDF polymeric solution and were forced towards co-axial nuzzles [10]. The flexibility of PZT/PVDF nanofiber films was observed in the optical image of the nanofiber films with a PZT content of 20 wt%, as shown in Fig. 2(b). This result confirms that the disadvantage of the previous technology, i.e., a loss of flexibility after the sintering process, was overcome.

The XRD patterns of the PZT/PVDF nanofibers prepared with different levels of PZT content are shown in Fig. 3. Although a PVDF peak was observed in PVDF nanofibers (PZT content of 0 wt%), rhombohedral perovskite (JCPDS #73-2022) PZT peaks and a PVDF peak coexisted in the XRD

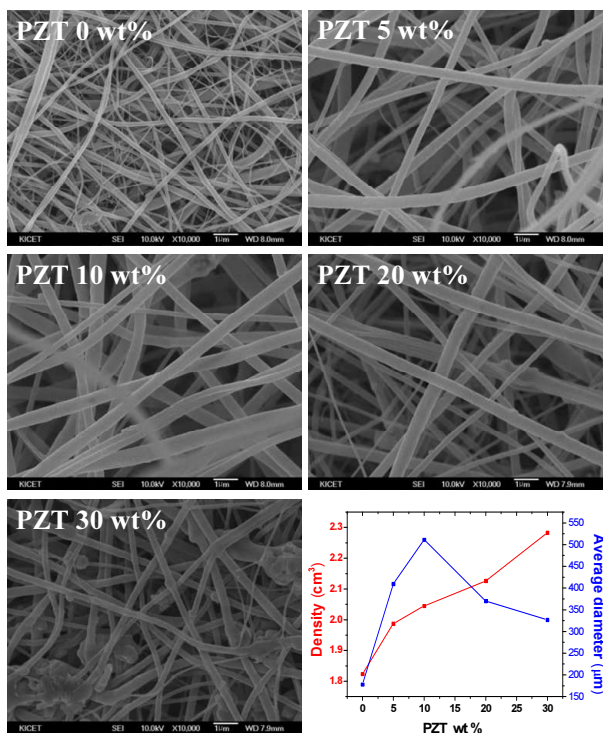


Figure 1. SEM images and the graphs of the density and diameter of the PZT/PVDF nanofibers prepared with different levels of PZT content

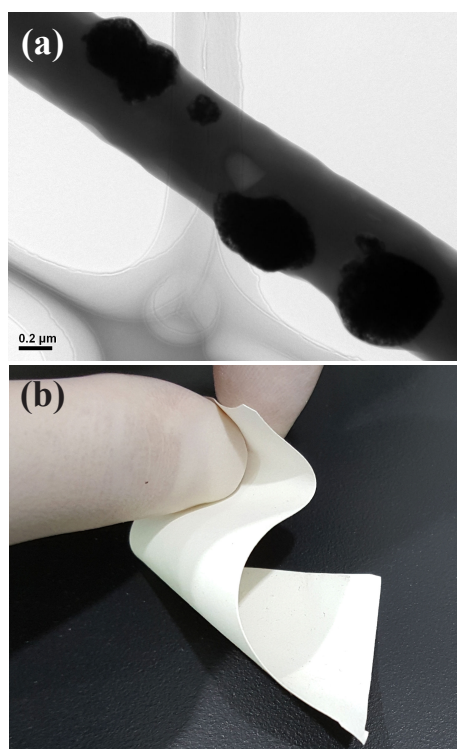


Figure 2. (a) TEM image and (b) optical image of the PZT/PVDF nanofiber films with a PZT content of 20 wt%

results of the PZT/PVDF nanofiber composites. Upon increasing the PZT content, the intensity of the perovskite peaks gradually increased and the intensity of the PVDF

peak gradually decreased. These results suggest that the perovskite structure of PZT is undisturbed during the composite part of the polymer and electrospinning process.

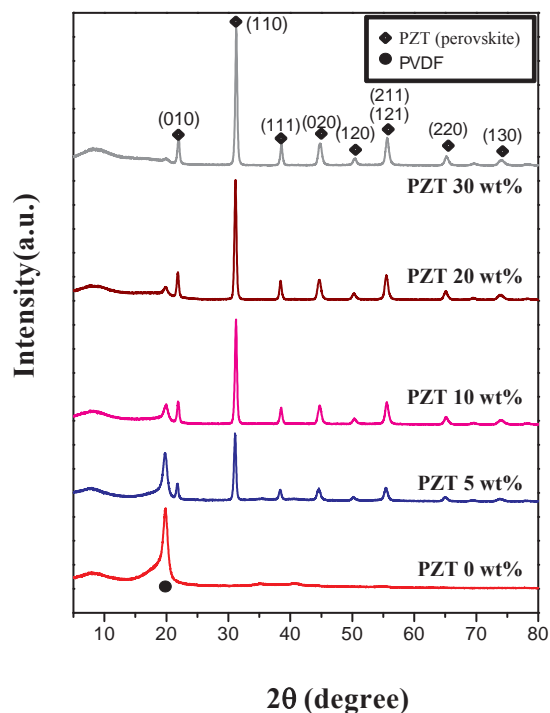


Figure 3. XRD patterns of the PZT/PVDF nanofibers prepared with different levels of PZT content

The tensile stress-strain properties of the PZT/PVDF nanofiber composite films prepared with different levels of PZT content were measured, as shown in Fig. 4. Young's modulus, defined as the ratio of the stress along an axis to the strain, reflects the bending stiffness of the actuator. The bending stiffness (B) for a cantilever beam type actuator is governed by the solid mechanics theory [11,12]: $B = EI/b$, where EI (E : Young's modulus, I : the moment of inertia) represents the flexural rigidity of a beam and b is the width of the beam. Young's modulus results for PZT/PVDF nanofiber composite films with PZT content of 0 wt%, 5 wt%, 10 wt%, 20wt% and 30 wt% were 79.4 MPa, 128.1 MPa, 1,131.5 MPa, 2,052.6 MPa and 89.2 MPa, respectively, as shown in the inset of Fig. 4. A better bending stiffness of PZT/PVDF nanofiber composites with a PZT content of 20 wt% can be expected with a higher Young's modulus.

The electric-field-induced polarization (P - E) of PZT/PVDF nanofiber composites prepared with different amounts of PZT was measured at room temperature and a frequency of 1 Hz, as shown in Fig. 5. The inset optical image of Fig. 5 is a PZT/PVDF nanofiber composite module with interdigitated electrodes for piezoelectric characteristics analysis. P - E hysteresis loops are necessary for validating the ferroelectric behaviour of a piezoelectric nanofiber material at a particular temperature and frequency. In the PZT/PVDF nanofiber composite module with a PZT content of 20 wt%, the highest value for P_{max} (maximum

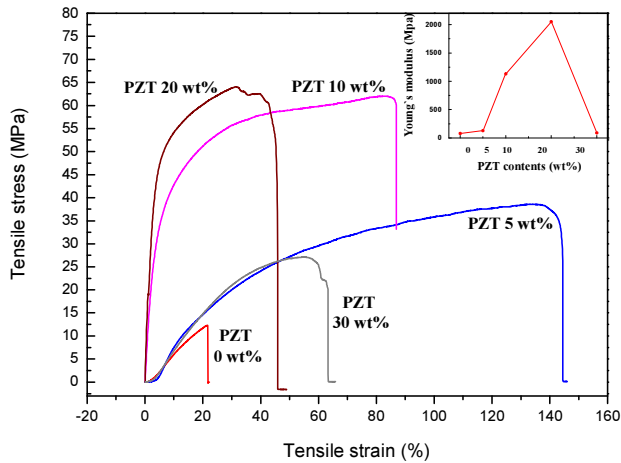


Figure 4. Tensile stress-strain properties of PZT/PVDF nanofiber composite films prepared with different levels of PZT content. The inset shows the results of Young's modulus for PZT/PVDF nanofiber composite films.

polarization) of $2.64 \mu\text{C}/\text{cm}^2$ was observed at $4 \text{ kV}/\text{mm}$. An increased P_{max} of 27 % was observed from pure PVDF nanofiber (PZT 0 wt%) of $2.08 \mu\text{C}/\text{cm}^2$ to PZT/PVDF nanofiber (PZT 20 wt%) of $2.64 \mu\text{C}/\text{cm}^2$. An increased P_r (remnant polarization) of 60 % was observed from pure PVDF nanofiber (PZT 0 wt%) of $0.15 \mu\text{C}/\text{cm}^2$ to PZT/PVDF nanofiber (PZT 20 wt%) of $0.24 \mu\text{C}/\text{cm}^2$. The results confirm that there is an optimal PZT amount (a weight ratio of 20 wt%) of PZT/PVDF nanofiber composites to achieve higher piezoelectric characteristics.

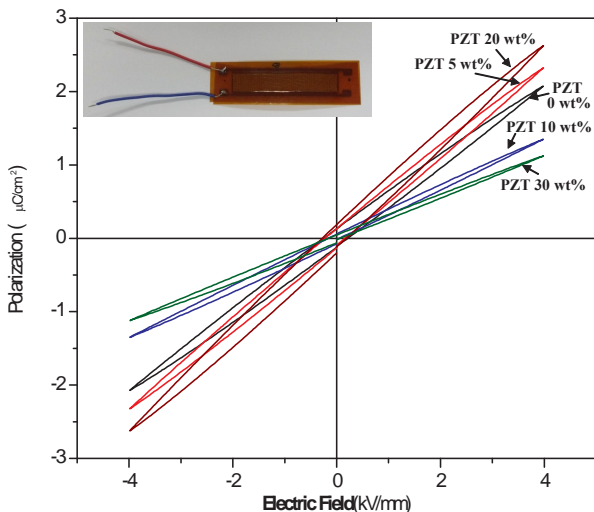


Figure 5. P-E hysteresis loops of PZT/PVDF nanofiber composites prepared with different levels of PZT content. The inset shows an optical image of a PZT/PVDF nanofiber composite module.

4. Conclusion

For the fabrication of PZT/PVDF nanofiber composites, sintered PZT ceramic powder and PVDF polymer were dispersed in DMF and acetone solvent and nanofiber composites were prepared by electrospinning. The XRD

measurements and TEM result indicated that the characteristics of PZT and PVDF coexisted in the PZT/PVDF nanofiber composites. The SEM observation showed that the PZT ceramic powder was present separately without mixing with the polymer in PZT/PVDF nanofibers with PZT 30 wt% and that there was an optimal PZT content for preparing PZT/PVDF nanofiber composites. PZT/PVDF nanofiber composites with PZT content of 20 wt% had enhanced mechanical and piezoelectric characteristics of Young's modulus ($2,052.6 \text{ MPa}$), P_{max} ($2.64 \mu\text{C}/\text{cm}^2$) and P_r ($0.24 \mu\text{C}/\text{cm}^2$).

5. Acknowledgements

This work was supported by a grant from the R&D programme funded by the Korea Institute of Ceramic Engineering and Technology (KICET).

6. References

- [1] Maeda R, Tsaur J J, Lee S H, Ichiki M (2004) Piezoelectric Microactuator Devices. *J. Electroceram.* 12:89.
- [2] Hsu Y C, Wu C C, Lee C C, Cao G Z, Shen I Y (2004) Demonstration and characterization of PZT thin-film sensors and actuators for meso- and micro-structures. *Sens. Actuator A* 116:369.
- [3] Chen X, Xu S, Yao N, Shi Y (2010) 1.6 V Nanogenerator for Mechanical Energy Harvesting Using PZT Nanofibers. *Nano Lett.* 10:2133.
- [4] Sobocinski M, Leinonen M, Juuti J, Mantyniemi N, Jantunen H (2014) A co-fired LTCC-PZT monomorph bridge type acceleration sensor Original. *Sens. Actuator A* 216:370.
- [5] Kozuka H, Takenaka S, Tokita H, Okubayashi M (2004) PVP-assisted sol-gel deposition of single layer ferroelectric thin films over submicron or micron in thickness. *J. Eur. Ceram. Soc.* 24:1585.
- [6] Alkoy E M, Dagdeviren C, Papila M (2009) Processing conditions and aging effect on the morphology of PZT electrospun nanofibers, and dielectric properties of the resulting 3-3 PZT/Polymer Composite. *J. Am. Ceram. Soc.* 92:2566.
- [7] Khajelakzay M, Taheri-Nassaj E (2012) Synthesis and characterization of $\text{Pb}(\text{Zr}_{0.52}\text{Ti}_{0.48})\text{O}_3$ nanofibers by electrospinning, and dielectric properties of PZT-Resin composite. *Mater. Lett.* 75:61.
- [8] Yun J S, Park C K, Cho J H, Paik J H, Jeong Y H, Nam J H, Hwang K R (2014) The effect of PVP contents on the fiber morphology and piezoelectric characteristics of PZT nanofibers prepared by electrospinning. *Mater. Lett.* 137:178.
- [9] Li D, Xia Y (2004) Electrospinning of nanofibers: reinventing the wheel? *Adv. Mater.* 16:1151.
- [10] Ashrafi F, Malekfar R, Babanejad S A, Norouzi M (2014) Synthesis of Titanium Dioxide Shell-Core

Ceramic Nano Fibers by Electrospin Method. Int. J. Chem. Tech. Res. 6:807.

- [11] Wang X L, Oh I K, Cheng T H (2010) Electro-active polymer actuators employing sulfonated poly(styrene-ran-ethylene) as ionic membranes. Polym. Int. 59:305.

- [12] Wyser Y, Pelletier C, Lange J (2001) Predicting and determining the bending stiffness of thin films and laminates. Pack. Technol. Sci. 14:97.